



TECHNICAL ARTICLE

Facile Electrochemical Fabrication of Pt Decorated rGO and Its Electro-Catalytic Applications

GENGAN SARAVANAN ^{1,2,4} R.M. GNANAMUTHU,¹
and SANJAY SANKARANARAYANAN³

1.—Department of Chemistry, Saveetha School of Engineering, Saveetha Institute of Medical and Technical Sciences, Saveetha University, Chennai, Tamil Nadu 602105, India. 2.—Yonsei University, 50 Yonsei-ro, Sinchon-dong, Seodaemun-gu, Seoul 120749, South Korea. 3.—Department of ECE, Koneru Lakshmaiah Education Foundation, Hyderabad, Aziz Nagar, Telangana 500075, India. 4.—e-mail: saravanan3che@gmail.com

A simplistic electrochemical advance has been developed for the synthesis of platinum with three different shapes: spherical (PtNPs-S), hierarchical (PtNPs-H), and dendritic (PtNPs-D) nanoparticles decorated electrochemically reduced graphene oxide (rGO) sheets on glassy carbon electrode (GCE) using a simple electrochemical deposition process. The electrochemical measurements and surface morphology of modified electrode were studied using cyclic voltammetry (CV), XRD, SEM, TEM, EDS, XPS, and FTIR analysis. The presence of rGO enhances wide spreading of Pt nanoparticles without agglomeration. Among different Pt shaped nanoparticles, PtNPs-H modified electrode showed better electrocatalytic properties in KOH medium.

INTRODUCTION

The development of non-enzymatic glucose electrooxidation is important in the field of medical diagnostics and the food processing industry.¹ Since C. Chen's pioneering work, progress in glucose electrooxidation has been one of the most active areas of research.² Due to its great selectivity, a glucose oxidase (GOX) enzyme-based electrode is commonly employed to develop electrooxidation of glucose and electrochemical sensors.³ However, enzyme-modified electrodes have several disadvantages, including low stability, expensive glucose oxidase (GOX) enzymes, demanding working conditions, and a time-consuming immobilization technique. Non-enzymatic electrooxidation processes have been developed because enzymes are affected by temperature and pH, usage of toxic chemicals, expensive enzyme isolation processes, and purification methodologies.^{4,5} Direct electrooxidation of glucose on several metal substrates including platinum, gold, palladium,^{6–8} and Pt, Pd, and Rh alloys

has been explored for non-enzymatic glucose electrooxidation.^{9–11} In any scenario, the enzyme-based electrode will be harmed, with low sensitivity, poor selectivity, and poisoning by absorbed anions, resulting in activity loss.¹² Due to their superior electron transport and electrocatalytic characteristics, Pt nanoparticles of various shapes have fascinated researchers¹³ and also been investigated to improve the electrocatalytic function on reduced graphite oxide (RGO), which acts as a better anchoring site for metal nanoparticles.¹⁴ Because of its outstanding electrical, optical, and chemical characteristics, rGO has been widely employed in nanomaterials and nanotechnology in recent years.^{15–17} The enormous specific surface area of the 2D rGO allows metal nanoparticles and composite materials to be supported. Because each atom in graphite oxide can also be a surface atom, adsorbed molecules benefit greatly from molecular interactions and hence electron transport via graphite oxide.¹⁸ Due to its excellent physical chemical properties, when graphite oxide is used to modify an electrode, it may promote electron transfer reactions;¹⁹ therefore, rGO is expected to become a more viable electrocatalyst carrier that can be used for electrooxidation of ascorbic acid, H₂O₂, and hydrazine.^{16,20–22} rGO with excellent physicochemical

(Received August 13, 2021; accepted March 14, 2022;
published online April 4, 2022)

properties can act as better support for Pt nanoparticles, thereby effectively transferring electrons from/to glucose for electrooxidation. For glucose electrooxidation, shape-dependent PtNPs-S, PtNPs-H, and PtNPs-D Pt nanoparticles with rGO modified electrodes were examined.

We demonstrated electrocatalytic behavior of three differently shaped Pt nanoparticles toward the non-enzymatic glucose oxidation current magnitude; among the three Pt nanoparticle modified electrodes, PtNPs-H was approximately 2–3 times higher than that of PtNPs-S and PtNPs-D modified electrodes. Differently shaped Pt nanostructures can be prepared by electrochemical deposition with different electrolyte compositions and times as well as either potential or current controlled methods. X-ray diffraction (XRD), scanning electron microscopy (SEM), and transmission electron microscope (TEM) were used to analyze the PtNPs-S, PtNPs-H, and PtNPs-D. Among the three shapes, PtNPs-H modified GCE has nearly 3–4 times higher current density than PtNPs-S and PtNPs-D electrodes.

EXPERIMENTAL

Preparation of Graphite Oxide (GO)

Graphite powder (Sigma Aldrich, USA), K_2PtCl_6 , glucose (Merck, Germany), KCl, sodium dodecyl sulfate, $NaNO_3$, Na_2SO_4 (Fisher Scientific USA), H_2SO_4 (China Reechemprivate Ltd.), $KMnO_4$ (India SD Fine Chemical), H_2O_2 (India Sarabhaichem), C_2H_5OH , acetone, and CH_3OH (SRL, Pvt. Ltd., India) can be used without further purification. Modified Hummer's method was adopted for graphite oxide synthesis; the complete preparation and electrochemical reduction of graphite oxide are as illustrated in Supplementary material SM 1.¹⁴

Preparation of rGO by Electrochemical Reduction

Because of the negatively charged surface of GO, the resulting uniform yellow-brown GO solution can be stable for a few months; 5 μ L of GO + 0.1% Nafion solution that was cast on the prepolished glossy carbon (GC) working electrode was allowed to dry in air overnight. In an aqueous 0.1 M Na_2SO_4 solution, electrochemical reduction of GO modified GCE was carried out in a three-electrode cell with Ag/AgCl and Pt foil as the reference and counter electrodes, respectively (Supplementary material SM 2).

Electrochemical Preparation of PtNPs-S, PtNPs-H, and PtNPs-D Modified Electrodes

PtNPs-S, PtNPs-H, and PtNPs-D were electrodeposited on previously produced rGO/GCE electrodes in 1.0 mM H_2PtCl_6 containing 0.02 M KCl, 0.5 M H_2SO_4 , and 1 mM SDS, respectively. After electrodeposition, the Pt electrode was repeatedly cleaned with Millipure MilliQ water and dried at

100°C for 1 min. The Pt loading on rGO/GCE was measured by a charge integrated during the Pt deposition, assuming a 100% current efficiency; charges for PtNPs-S, PtNPs-H, and PtNPs-D are 0.0328, 0.0394, and 0.0454 C equivalents, which are equivalent to platinum loadings of 17 μ g, 19.8 μ g, and 22.9 μ g, respectively (Supplementary material SM 3).

Characterization of GO, rGO PtNPs-S, PtNPs-H, and PtNPs-D Nanoparticles

Electrochemical experiments were conducted in a conventional three-electrode system using the PARSTAT 2273 (Princeton Applied Research Corporation) electrochemical workstation, purity 99.99%; a Pt foil (1 cm^2), glassy carbon electrode (2 mm diameter), and saturated Ag/AgCl electrode were employed as the counter, working, and reference electrodes, respectively. The FT-IR spectra were obtained using a PerkinElmer spectrum GX FT-IR system with pure KBr as the background. X-ray photoelectron spectroscopy (XPS) of GO and rGO was investigated using VG electron spectroscopy. All spectra were recorded using an x-ray source (Al K_{α} radiation, $E = 1486$ eV) with a scan range of 0–1200 eV binding energy. The collected high-resolution XPS spectra were analyzed using the XPS peak fitting software program. The x-ray diffraction pattern of the crystal phase was measured using a Phillips diffractometer, during which Cu K_{α} was used to form 2θ from 10° to 80°, $\lambda = 0.154$ nm. Surface morphologies of GO, rGO, PtNPs-S, PtNPs-H, and PtNPs-D nanoparticles were examined using a scanning electron microscope (Hitachi, 3000H) and TEM using Tecnai 20 G2 (FEI brand).

RESULTS AND DISCUSSION

Electrochemical Reduction of Graphite Oxide

GO-modified GCE, saturated Ag/AgCl, and Pt foils are used as working, reference, and counter electrodes, respectively, in a 0.1 M Na_2SO_4 solution by extended cyclic voltammetry from +1.0 V to –1.1 V for electrochemical reduction of GO.¹⁴ The FT-IR spectrum of the GO sample indicates the presence of epoxy (~ 1226 cm^{-1}), carbonyl (1415 cm^{-1}), carbonyl C=O (1720 cm^{-1}), and hydroxide (3420 cm^{-1}) functional groups. The dramatic fall in peak intensity at 1226 cm^{-1} , 1415 cm^{-1} , 1720 cm^{-1} , and 3420 cm^{-1} , which shows that graphite oxide has been effectively reduced to rGO by electrochemical reduction, demonstrates the accompanying reduction in rGO.²³

Structure and Morphology

Graphite oxide and reduced graphite oxide are studied using the FT-IR spectrum of the GO sample (Supplementary material SM 4), which indicates the presence of C=O (1720 cm^{-1}), carbonyl (1415 cm^{-1}), OH (3420 cm^{-1}), and epoxy resin

($\sim 1226\text{ cm}^{-1}$) functional groups. The concomitant reduction in rGO can be demonstrated by the sharp decrease in peak intensity at $\sim 3420\text{ cm}^{-1}$, $\sim 1720\text{ cm}^{-1}$, $\sim 1415\text{ cm}^{-1}$, and $\sim 1226\text{ cm}^{-1}$, which indicates that graphite oxide has been successfully reduced to graphite oxide by electrochemical reduction.²³ X-ray photoelectron spectroscopy (XPS) (Omicron ESCA probe) of graphite oxide's C 1s XPS spectrum (Supplementary material SM 5-8) reveals a high degree of oxidation with four components,²⁴ that is, non-oxidized ring C (284.2 eV) and C in the C-O bond (286.4 eV), and the carbonyl C (C=O, 287.5 eV) is thus the carboxylate carbon (O=C-O, 289.2 eV). Carbonyl C (C=O, 287.5 eV) and therefore carboxylate carbon (O=C-O, 287.2 eV) are non-oxidized ring C (284.2 eV), C-O bond C (286.4 eV), carbonyl C (C=O, 287.5 eV), and thus carboxylate carbon (O=C-O, 287.2 eV).²⁵ The corresponding oxygen functionality associated with graphite oxide may be seen in the C 1s XPS spectra of reduced graphite oxide. After reduction, the height strength of those components in the sample is substantially lower than that of graphite oxide, suggesting that there has been a lot of deoxidation during the reduction process. The corresponding oxygen functionality associated with graphite oxide may be seen in the reduced graphite oxide C 1s XPS spectrum. After reduction, the height strength of those components in the sample is substantially lower than in graphite oxide, indicating that there was a lot of deoxidation during the reduction process.

The C/O ratio in the reduced graphite oxide material (5.3) and the C/O ratio in the beginning graphite oxide material (2.6) were determined using XPS measurements. As a result, reduced graphite oxide is commonly described as being made up of partly oxidized graphite nanosheets if a significant quantity of oxygen exists after reduction. The increased GO's black color indicated the portion of graphite oxide that had been converted to re-graphitized, which was consistent with other reports.^{26,27} A Phillips diffractometer was used to measure the x-ray diffraction pattern of PtNPs rGO composites; Cu K α from 10° to 80° was employed throughout this scan time, with $a = 0.154\text{ nm}$.

XRD patterns are used to investigate the crystal characteristics of electrodeposited PtNPs-S, PtNPs-H, and PtNPs-D nanoparticles on Si wafer as illustrated in Fig. 1A (green), Peaks 69.15 and 10 for PtNPs-S (220) and rGO carbon (002), respectively. For PtNPs-H there were three peaks, (002), (111), and (311), corresponding to 23.42, 42, and 78, respectively [Fig. 1A (black)]. Similarly for PtNPs-D, three plane (002), (111), and (311) peaks were observed at 26, 42.6, and 76 corresponding to graphite oxide carbon and Pt, respectively [Fig. 1 (red)].

The surface morphologies of GO, rGO, PtNPs-S, PtNPs-H, and PtNPs-D nanoparticles were examined by SEM as shown in Supplementary materials

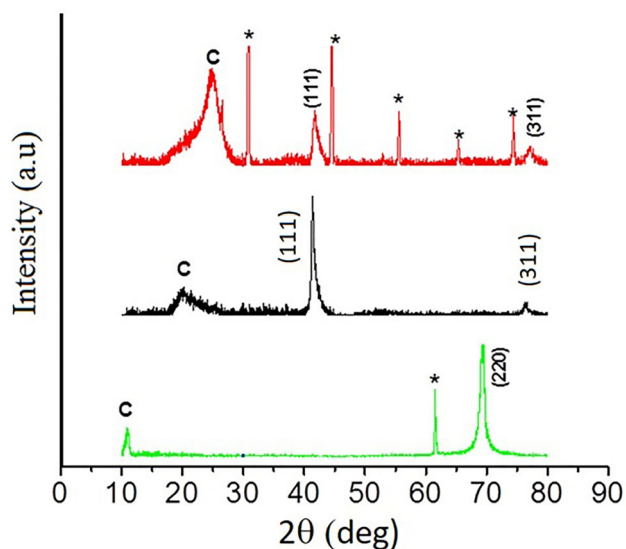


Fig. 1. Typical XRD patterns of PtNPs-S (green), PtNPs-H (black), and PtNPs-D (red) nanoparticles electrodeposited on previously drop-cast GO suspension and electro-reduced to rGO on Si wafer (*Si wafer substrate peak) (Color figure online).

SM 9-13. GO and rGO nanosheets (Supplementary material SM 9 and 10) were entirely exfoliated and distributed, and rGO restoration showed characteristic wrinkles according to the findings. Electrodeposited PtNPs-S, PtNPs-H, and PtNPs-D nanoparticles on rGO undergo electrochemical reduction in the metal ion precursor solution, resulting in the formation of metal nanoparticle deposition on it (Supplementary material SM 11, 12, and 13). The SEM picture reveals well-dispersed PtNPs-S with multi-faceted characteristics, with most of their forms being spherical with a diameter of roughly 52 nm. PtNPs-H nanoflowers have many petal-like nanosheets with a diameter of 55 nm, which may significantly increase the electrocatalyst specific surface area and increase PtNP hierarchy use. SEM pictures demonstrated that branches were radically orientated with progressively increasing size from center point to outer circumference in a uniform sized particle of 58 nm (Supplementary material SM 13). The EDS spectra of rGO modified GCE with electrodeposited PtNF/rGO are shown in Fig. 2, with C, O, and Pt concentrations of 73.05%, 19.80%, and 7.15%, respectively, based on EDX data. Figure 3 showed a typical $i-t$ curve for the electrochemical deposition of Pt on reduced GO on GCE with an applied potential of -0.2 V in $1\text{ mM H}_2\text{PtCl}_6$ in $0.5\text{ M H}_2\text{SO}_4$ for about 200 s.

Electrochemically synthesized PtNPs-S, PtNPs-H, and PtNPs-D nanoparticles dispersed in acetone under ultrasonic conditions about 10 min for TEM characterization. TEM image of rGO sheet revealed a folded filamentous form with many wrinkles, which can prevent electrodes from being stacked closely face to face, so it is preferable to make full use of the high surface area as shown in Fig. 4. The

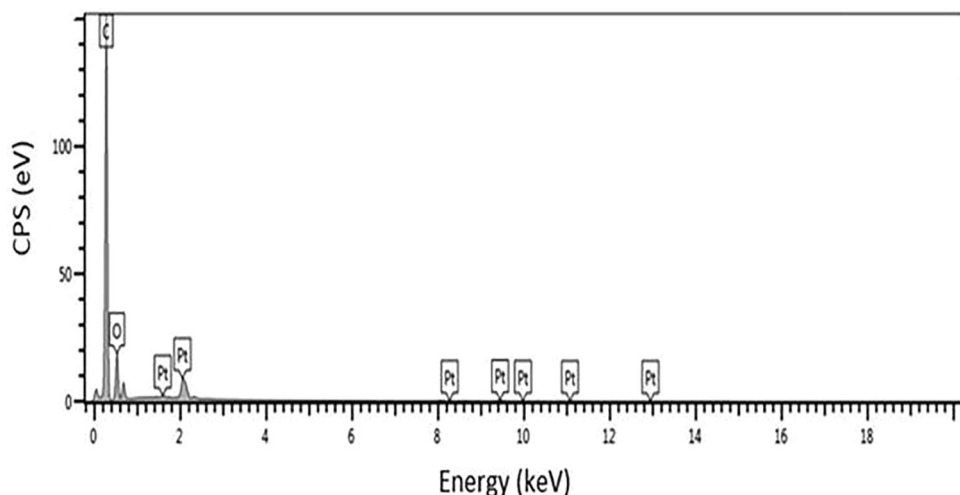


Fig. 2. EDS spectrum of the exfoliated graphene supported PtNF/rGO.

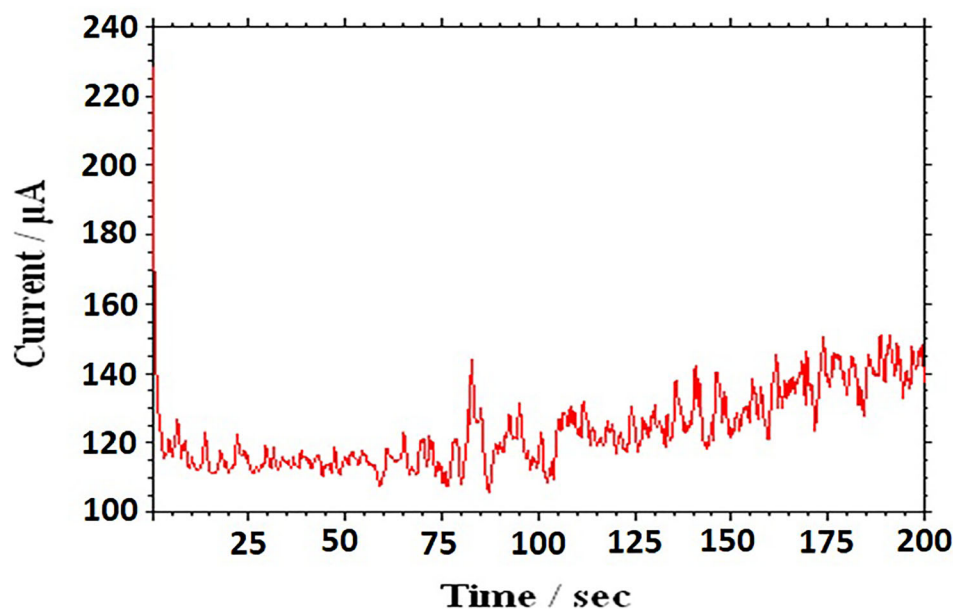


Fig. 3. Typical *i-t* curve for the electrochemical deposition of Pt on reduced GO on GCE with an applied potential of -0.2 V in 1 mM H_2PtCl_6 in 0.5 M H_2SO_4 for about 200 s.

rGO provides better anchoring supports to PtNPs-S, PtNPs-H, and PtNPs-D nanoparticles, occupying the surface of the rGO sheet, preventing aggregation and re-stacking. Shape controlled synthesized PtNPs-S, PtNPs-H, and PtNPs-D nanoparticles are depicted in TEM Figs. 5, 6, and 7. These images also reveal that nanoparticles are evenly dispersed, with average particle sizes of (50–70 nm), (50–80), and (55–80) for PtNPs-S, PtNPs-H, and PtNPs-D, respectively. In the absence of agglomeration, surface functional groups such as $-\text{OH}$ and $\text{C}=\text{O}$ are anchoring sites for metal NPs on rGO sheets, indicating that those regions are too important to demonstrate increased catalytic activity.

Electrooxidation of Glucose Using PtNPs-S, PtNPs-H, and PtNPs-D Modified Electrodes

PtNPs-S, PtNPs-H, and PtNPs-D modified electrodes were subjected to electrooxidation of glucose from -1.0 V to 0.6 V using 0.5 M KOH and 0.5 M KOH + 0.1 M glucose solution; all potentials referred to the Ag/AgCl (saturated KCl) unless otherwise stated.²⁸ In alkaline solution, the CV Figure illustrates the hydrogen adsorption (1.0 – 0.55 V), double layer (0.55 – 0.25 V), and oxide formation region (0.5 – $+0.2$ V) of the PtNP-H-modified electrode. Adsorption occurs in most electrocatalytic reactions, when reactant molecules adsorb onto the

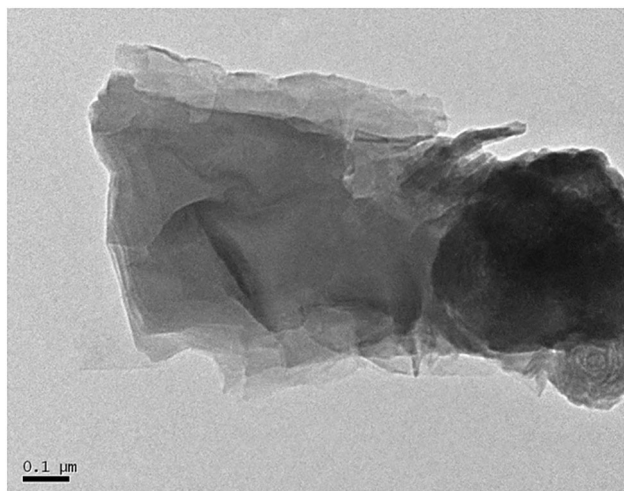


Fig. 4. TEM image of rGO.

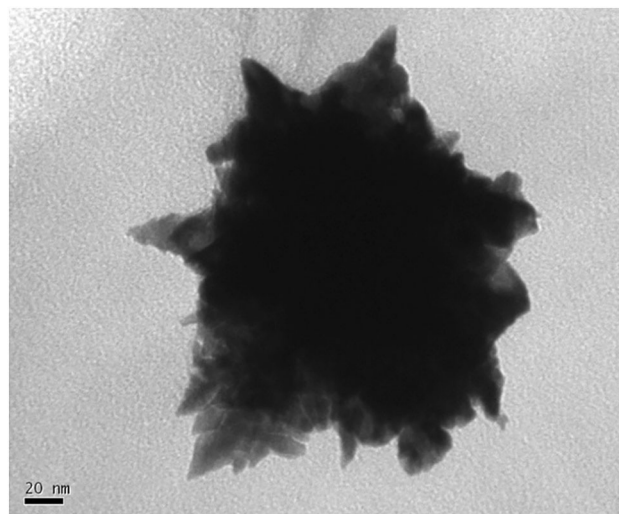


Fig. 7. TEM image of PtNPs-D.

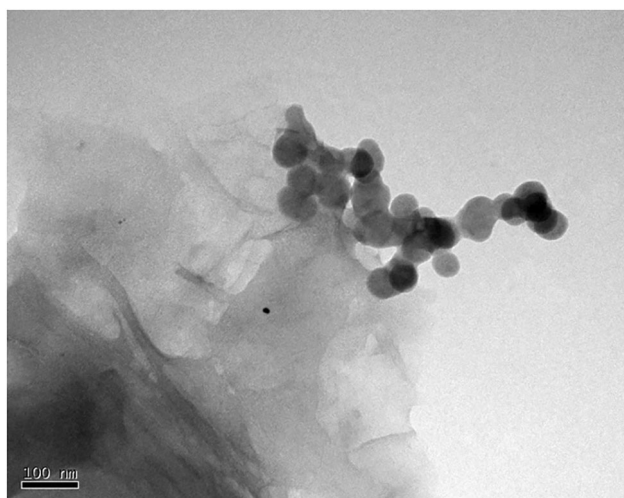


Fig. 5. TEM image of PtNPs-S.

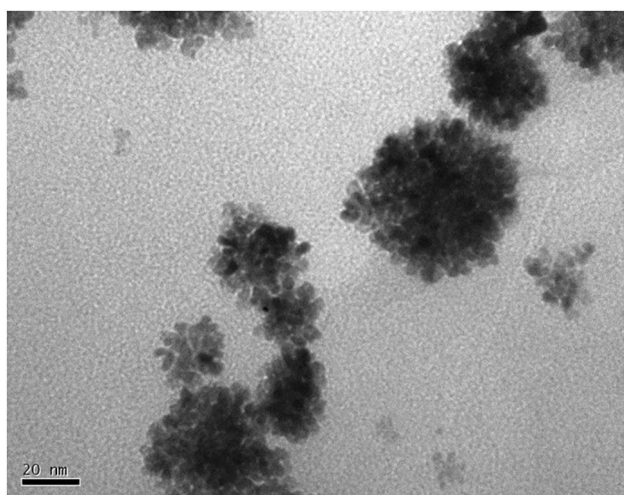


Fig. 6. TEM image of PtNPs-H.

electrode's active sites, which depends on redox center electronic states, empty *d*-orbitals at transition metal, and defects at catalysts. Adsorption of glucose, bond breaking, and production of intermediates leads to changing oxidation state of the redox center, and hence contact between the product and electrode decreases resulting in desorption of the reaction product from the electrode surface. As the glucose molecule approaches the electrode, the chemical contact between C-1 and its hydrogen atom at the electrode surface increases, resulting in dehydrogenation at C-1 and adsorption on electrode surface.

Figure 8 shows three distinct oxidation peaks for glucose electrooxidation from a negative to a positive potential: O1, O2, and O3.²⁹ At -0.68 V potential, the electrooxidation peak O1 arises owing to chemisorptions and dehydrogenation of glucose; this peak corresponds with the platinum electrode's hydrogen desorption peak (Eq. 1). The gluconate peak O2 at -0.27 V arises at OH- adsorbed catalyst surface by direct glucose oxidation from the majority to gluconolactone, which on hydrolysis generates gluconate (Eq. 2). Peak O3 (at 0.18 V) is acquired on an already oxidized catalyst surface and should desorb from oxidized adsorbed residue (Eq. 3). The second oxidation peak at the O2 location is particularly noticeable, with higher current density than the O1 and O3 positions, which both have excessively low current density compared to the O2 for three modified electrodes. The cathode peak of the PtNP-H catalyst was seen in the negative going scan, and the cathode current peak R1 at -0.35 V in the positive potential scan may also be ascribed to the reduction of platinum oxide. The reduction peak R2 at -0.77 V might be attributable to glucose oxidation product desorption (reduction or oxidation).³⁰ The current density obtained matching the surface area normalized value as well as electrooxidation of glucose in alkaline medium is utilized to

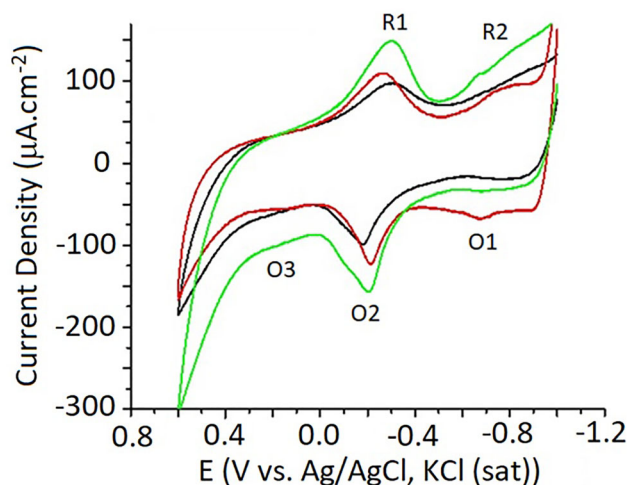
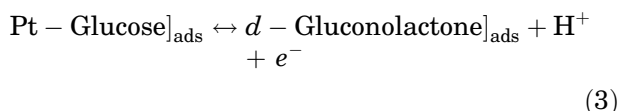
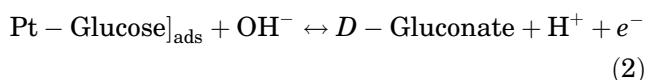
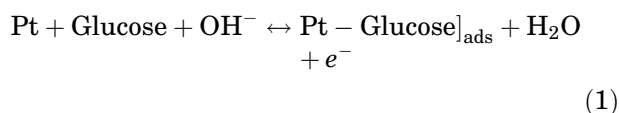


Fig. 8. Cyclic voltammogram of glucose electro-oxidation on PtNPs-S, PtNPs-H, and PtNPs-D modified electrodes starting from -1 V to 0.6 V in 0.5 M KOH and 0.1 M glucose solution at a scan rate of 50 mV s^{-1} .

power glucose fuel cells to assess the electrocatalytic tendency of Pt nanoparticles with varied shapes.



The electrocatalytic activity of PtNPs-S, PtNPs-H, and PtNPs-D modified electrodes was evaluated under similar experimental conditions as shown in Fig. 9 (enlarged CV) from 0.6 V to 1.0 V. Chemisorptions of glucose at OH-adsorbed Pt (111) plane are connected to the initial voltametric peak, and electrooxidation depends on Pt nanoparticle crystallographic planes, shape, and OH- and glucose adsorption at Pt sites.³¹ PtNPs-H had higher current densities at O2 than PtNPs-S and PtNPs-D modified electrodes; catalytic current density of PtNPs-H electrode is two times that of PtNPs-S and 1.2 times that of PtNPs-D. As indicated in Fig. 1 (black), PtNPs-H had high intensity (111) planes that had lower intensities at PtNPs-S and PtNPs-D nanoparticle planes. The initial oxidation peak current density of O1 for PtNPs-H electrode is -31.1 μA , which is lower than for PtNPs-D (-68.6 μA) but greater than for PtNPs-S (-12.5 μA) modified electrodes. As a result, PtNPs-H has a moderate adsorption behavior compared to PtNPs-S and PtNPs-D modified electrodes, which is an important attribute for electrocatalyst.

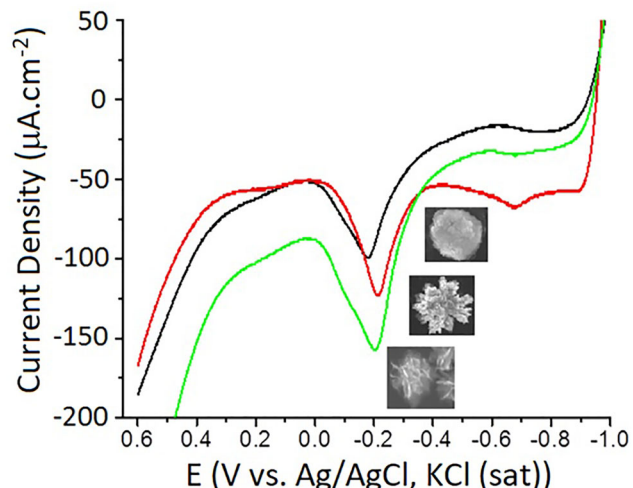


Fig. 9. Enlarged CV curve region from -1.00 V to 0.6 V.

PtNPs-Hs have a gap amid their unsymmetrical petals, according to a SEM picture at higher magnification (Supplementary material SM 12 inset). This allows for rapid access to the electrolyte, resulting in a larger electrode surface area. The electrocrystallization of metals on a different substrate starts on high-energy surface sites, and it has been discovered that electrodeposited PtNPs-H has more surface defects, short branches, kinks, steps, and terraces, all of which favor electronucleation of metal particles over growth.³²

Stability of PtNPs Hierarchical-rGO/GCE Modified Electrodes

It is important to note that each of the three types—PtNPs-S, PtNPs-H, and PtNPs-D—can retain high stability during glucose electrooxidation. Current densities of all peaks for PtNPs-H modified electrodes maintain a minimum of 90% of their initial values after several potential cycles (~ 100 No's) for potentials of 0.4 V, 0.10 V, and 0.25 V (Supplementary material SM 14 and 15) because of the superior features of PtNPs-H modified electrodes for non-enzymatic glucose electrooxidation.

CONCLUSION

In conclusion, we adopted a very simple electrodeposition approach to successfully produce PtNPs-S, PtNPs-H, and PtNPs-D modified electrodes. Among three electrodeposited nanoparticles, PtNPs-H contains abundant surface imperfections, such as branches, kinks, steps, and terraces, which enhance accessibility of glucose molecules for better electrooxidation. Because of the synergistic effects of both rGO and PtNPs-H, with demonstrated better electrooxidation glucose, the PtNPs-H modified

electrode is a good candidate for non-enzymatic glucose electrooxidation and also has very good stability even after many cycles.

ACKNOWLEDGEMENTS

The authors wish to express their sincere thanks to the Principal, Director, Dean, Saveetha School of Engineering Chennai, for constant encouragement.

CONFLICT OF INTEREST

The authors declare that they have no known competing financial interests or personal relationships that could have appeared to influence the work reported in this paper.

SUPPLEMENTARY INFORMATION

The online version contains supplementary material available at <https://doi.org/10.1007/s11837-022-05269-1>.

REFERENCES

- J.D. Newman and A.P.F. Turner, *Biosens Bioelectron* 20, 2435. (2005).
- L.C. Clark Jr., C. Lyons, and J. Ann, *N.Y. Acad. Sci.* 102, 29. (1962).
- C.Y. Deng, J.H. Chen, X.L. Chen, C.H. Mao, L.H. Nie, and S.Z. Yao, *Biosens. Bioelectron.* 23, 1272. (2008).
- Y. Wen, W. Meng, C. Li, L. Dai, Z. He, L. Wang, M. Li, and J. Zhu, *Dalton Trans.* 47, 3872. (2018).
- K.E. Toghiani and R.G. Compton, *Int. J. Electrochem. Sci.* 5, 1246. (2010).
- S. Park, T.D. Chung, and H.C. Kim, *Anal. Chem.* 75, 3046. (2003).
- S. Cherevko and C.-H. Chung, *Sens. Actuators B: Chem.* 142, 216. (2009).
- H. Bai, M. Han, Y. Du, J. Bao, and Z. Dai, *Chem. Commun.* 46, 1739. (2010).
- Y. Sun, H. Buck, and T.E. Mallouk, *Anal. Chem.* 73, 1599. (2001).
- S. Park, H. Boo, and T.D. Chung, *Anal. Chim. Acta.* 556, 46. (2006).
- J. Wang, D.F. Thomas, and A. Chen, *Anal. Chem.* 80, 997. (2008).
- Y.B. Vassilyev, O.A. Khazova, and N.N. Nikolaeva, *J. Electroanal. Chem. Interfacial Electrochem.* 196, 105. (1985).
- V. Komanicky, H. Iddir, K.-C. Chang, G. Karapetrov, D. Hennessy, and P. Zapol, *J. Am. Chem. Soc.* 131, 5732. (2009).
- G. Saravanan and S. Mohan, *Appl. Surf. Sci.* 386, 96. (2016).
- K.S. Novoselov, A.K. Geim, S.V. Morozov, D. Jiang, Y. Zhang, S.V. Dubonos, L.V. Grigorieva, and A.A. Firsov, *Science* 306, 666. (2004).
- M. Zhou, Y. Zhai, and S. Dong, *Anal. Chem.* 81, 5603. (2009).
- C.S. Shan, H.F. Yang, J.F. Song, D.X. Han, A. Ivaska, and L. Niu, *Anal. Chem.* 81, 2378. (2009).
- M. Pumera, A. Ambrosi, A. Bonanni, E.L.K. Chng, and H.L. Poh, *Anal. Chem.* 29, 954. (2010).
- J. Lu, F. Do, L.T. Drzal, R.M. Worden, and I. Lee, *ACS Nano* 2, 1825. (2008).
- J. Wang, S. Yang, D. Guo, P. Yu, D. Li, J. Ye, and L. Mao, *Electrochem. Commun.* 11, 1892. (2009).
- W.I. Lin, C.S. Liao, J.H. Jhang, and Y.C. Tsai, *Electrochem. Commun.* 11, 2153. (2009).
- Y. Wang, Y. Wan, and D. Zhang, *Electrochem. Commun.* 12, 187. (2010).
- S.Y. Wang, D.S. Yu, L.M. Dai, D.W. Chang, and J.B. Baek, *ACS Nano* 5, 6202. (2011).
- S. Stankovich, R.D. Piner, X. Chen, N. Wu, S.T. Nguyen, and R.S. Ruoff, *J. Mater. Chem.* 16, 155. (2006).
- D. Briggs and G. Beamson, *High Resolution XPS of Organic Polymers: The Scienta ESCA300 Database* (Wiley, New York, 1992), p 295.
- A.B. Bourlinos, D. Gournis, D. Petridis, T. Szabo, A. Szeri, and I. Dekany, *Langmuir* 9, 6050. (2003).
- J. Yan, J. Liu, Z. Fan, T. Wei, and L. Zhang, *Carbon* 50, 2179. (2012).
- B. Beden, F. Largeaud, K.B. Kokoh, and C. Lamy, *Electrochim Acta.* 41, 701. (1996).
- G. Kokkinidis, J.M. Leger, and C. Lamy, *J. Electroanal. Chem.* 242, 221. (1988).
- L.-Q. Rong, C. Yang, Q.-Y. Qian, and X.-H. Xia, *Talanta* 72(2), 819. (2007).
- K.D. Popovic, N.M. Markovic, A.V. Tripkovic, and R.R. Adzic, *J. Electroanal. Chem. Interfacial Electrochem.* 313, 181. (1991).
- H.-W. Lei, B. Wu, C.-S. Cha, and H. Kita, *J. Electroanal. Chem.* 382, 103. (1995).

Publisher's Note Springer Nature remains neutral with regard to jurisdictional claims in published maps and institutional affiliations.